

GLOBAL WARMING AND SF₆ MOLECULE

UDC 53+504.055

J. Gajević¹, M. Stević¹, J. Nikolić², M. Rabasović², D. Markushev²

¹Mathematical High School, Kraljice Natalije 37, 11000 Beograd, Serbia & Montenegro

²Institute of Physics, Pregrevica 118, 11080 Beograd-Zemun,
Serbia & Montenegro, markusev@phy.bg.ac.yu

Abstract. *In this paper the basic SF₆ molecule physical characteristics are given concerning its influence on global warming and green house effect. Absorption and relaxation characteristics of this molecule have been investigated within the frame of nonlinear molecule – strong laser field interaction in different gas mixtures. All experiments have been performed on a different gas mixture pressures to analyze and investigate relaxation and energy transfer characteristics of absorbing molecules and non-absorbing collision partners. To show the SF₆ absorption and relaxation and energy transfer capability, comparison between SF₆ and C₂H₄ was given using the same experimental conditions and argon as a buffer gas. All measurement points and their calculated values presented in this paper have been obtained using the infrared-pulsed photoacoustics technique adopted for atmospheric and subatmospheric pressures.*

Key words: *multiphoton, laser, molecules, photoacoustics, environment, global warming, greenhouse effects, infrared.*

INTRODUCTION

In 1992, under the United Nations Framework Convention on Climate Change (UNFCCC), 186 countries agreed to develop and submit a national inventory of anthropogenic greenhouse gas emissions and sinks. To fulfill this obligation, each year hundreds of scientists and national experts collaborate in developing a set of methodologies and guidelines to help countries create inventories that are comparable across international borders.

Many chemical compounds found in the Earth's atmosphere act as greenhouse gases, trapping outgoing terrestrial radiation and warming the earth's atmosphere [1-8]. Some emissions of greenhouse gases occur naturally, while others result from human activities. Carbon dioxide, methane, nitrous oxide, and ozone are greenhouse gases that have both natural and human-related emission sources. In addition, humans have created other greenhouse gases, such as hydrofluorocarbons (HFCs), perfluorocarbons (PFCs), and

sulfur hexafluoride (SF_6). The global warming potential (GWP) of a greenhouse gas is the ratio of global warming, or radiative forcing, from the emission of one unit mass of a greenhouse gas, to that of one unit mass of carbon dioxide over a specified time horizon. Calculation of GWPs is based on the lifetime of the gas and how efficiently it traps heat in the atmosphere.

Emissions of greenhouse gases result from many of the industrial, transportation, agricultural, and other activities that take place in the urban areas. The following is a description of the various sectors that emit greenhouse gases.

Historically, *energy-related* activities have accounted for more than three-quarters of GWP-weighted greenhouse gas emissions. Most of these are carbon dioxide emissions; however, some emissions of methane and nitrous oxide also result from stationary and mobile combustion. Almost all emissions from the energy sector result from fossil fuel combustion, which includes the burning of coal, natural gas, and petroleum. Fossil fuel combustion from stationary sources, such as electricity generation, represents more than half of energy-related emissions, while combustion of fossil fuels by mobile sources, such as automobiles, represents approximately one-third. In addition to fossil fuel combustion-related activities, carbon dioxide is also emitted as a result of natural gas flaring and biomass burning, and methane is emitted through coal mining, as well as the production, processing, transmission, and distribution of natural gas and petroleum.

Industrial processes emit greenhouse gases as a by-product of various non-energy related industrial activities. Manufacture of cement, lime, soda ash, iron, steel, aluminum, ammonia, titanium dioxide, and ferroalloys produces carbon dioxide as a by-product. The consumption of limestone, dolomite, and carbon dioxide as raw materials in industrial applications also releases carbon dioxide emissions. The production of petrochemicals and silicon carbide results in small amounts of methane emissions, while producing nitric and adipic acid generates nitrous oxide emissions. Emissions of HFCs, PFCs, and SF_6 are particularly important as substitutes for ozone-depleting substances such as chlorofluorocarbons (CFCs). These gases may also be emitted as a result of aluminum and HCFC-22 production, semiconductor manufacturing, electrical transmission and distribution, and magnesium production and processing.

Agricultural activities contribute directly to emissions of methane and nitrous oxide. The majority of nitrous oxide emissions occur because cropping and fertilizer practices increase the quantity of reactive nitrogen in the soils. This occurs through application of commercial fertilizers, livestock manure, and sewage sludge; production of nitrogen-fixing crops and forages; retention of crop residues on the field; and the cultivation of soils high in organic matter. These activities make more nitrogen available for the generation of nitrous oxide through microbial activity. The normal digestive processes in ruminant livestock (known as enteric fermentation) account for the largest portion of methane emissions. The agriculture sector also emits methane and nitrous oxide from managed and unmanaged manure, rice cultivation, and the burning of agricultural residues.

The natural carbon fluxes between biomass, soils, and the atmosphere change when humans alter the terrestrial biosphere through land-use, changes in land-use, and forest management practices. Various forest, agricultural soil, and land management practices can result in the uptake (i.e., sequestration) or emission of carbon dioxide. If these activities result in a net removal of carbon dioxide (versus net emission), they can offset a portion of total greenhouse gas emissions each year. Forestlands, followed by agricultural soils, contribute the most to the net uptake of carbon dioxide.

Waste management and treatment activities are another source of greenhouse gas emissions in the urban areas. Landfills are the largest source of anthropogenic methane emissions. Wastewater treatment systems, including human sewage treatment, are sources of methane and nitrous oxide emissions.

Hydrofluorocarbons (HFCs), perfluorocarbons (PFCs), and sulfur hexafluoride (SF₆) are powerful greenhouse gases. HFCs are primarily used as replacements for ozone-depleting substances, but also are emitted as a by-product of the HCFC-22 manufacturing process. PFCs and SF₆ are emitted by a variety of industrial processes including aluminum smelting, electric power transmission and distribution, magnesium processing, and semiconductor manufacturing. Currently, HFCs, PFCs, and SF₆ have a relatively small aggregate radiative forcing impact; however, because some of them have long atmospheric lifetimes, their concentrations can irreversibly accumulate in the atmosphere [1-8].

PHYSICAL CHARACTERISTICS OF SF₆ MOLECULE

If one does not know the physical characteristics of sulfur hexafluoride (SF₆), it will be easy for him to consider SF₆ role in global warming and processes in atmosphere negligible. The real situation is completely different. The main physical quantities of this molecule, which could contribute to the understanding of why this molecule is a very good absorber and energy transfer partner, include [9-36]: absorption cross section σ , rotational to rotational (τ_{rot}) and vibrational to translational (τ_{v-T}) relaxation time. High values of σ , in linear and nonlinear regime of absorption [9-14], show its ability for easy radiation field – molecule interaction (especially infrared (IR) radiation field). Values of τ_{rot} in the range of $(1-2)\times 10^{-7}$ s [23-30] show its ability to reach proper ro-vibrational state due to mutual collisions with its gas partners, enhancing the absorption ability more than 50 %. Values of τ_{v-T} in the range of $(2-5)\times 10^{-6}$ s [19-22] show its ability to transfer absorbed energy from its vibrational to translational modes of its collisional partners efficiently. Recent measurements show that concentration of sulfur hexafluoride in atmosphere is 10^8 times less than concentration of more investigated main greenhouse gas CO₂. But, all experiments show that SF₆ molecule is a very good absorber of infrared radiation, and also a good collisionally induced energy transfer partner, especially on atmospheric pressure. Its absorption cross section and relaxation time (vibrational to translational and rotational to rotational) values indicate that, in both linear and nonlinear absorption regime, this molecule absorbs and transfers a large amount of energy for a wide range of radiation source energies and frequencies. According the IPCC 2001 Report [2], concentration of SF₆ in atmosphere is 4.2 parts per trillion (ppt), rate of concentration change is 0.24 ppt/year, atmospheric lifetime is 3,200 years and global warming potential (GWP) calculated over 100 year time horizon is 23,900. Comparing these SF₆ results with CO₂, especially for GWP, one can say that one molecule of SF₆ has the same influence as 23,900 molecules of CO₂. Having in mind the constant rising of SF₆ concentration in the atmosphere, its influence on global warming in the future must be taken into consideration [1-8].

Sulphur hexafluoride SF₆ is a gas that is used in electrical power equipment. It is colorless, odorless, non-flammable and chemically stable. This means that at room temperature it does not react with any other substance. Stability comes from the symmetrical arrangement of the six fluorine atoms around the central sulphur atom. And this stability

is just what makes the gas useful in electric equipment. SF₆ is a very good electrical insulator and can effectively extinguish arcs, which makes high and medium voltage apparatus filled with SF₆ highly popular. SF₆ can be found in millions of electric apparatus all over the world; electrical equipment containing SF₆ is a large export article. SF₆ is formed by a chemical reaction between molten sulphur and fluorine. Fluorine is obtained by the electrolysis of hydrofluoric acid (HF). Pure SF₆ is not poisonous. The gas is not dangerous to inhale, provided the oxygen content is high enough. In principle you can inhale a mixture of 20% oxygen and 80% SF₆ without danger. SF₆ is about 6 times heavier than air. That means that it may collect in cable ducts or at the bottom of tanks. The gas is not dangerous to inhale but if it does accumulate where people work, there is a risk of suffocation due to the lack of oxygen.

Sulfur atom has four stable isotopes characterized with their mass numbers 32, 33, 34 and 36, with their natural abundances 95%, 0.75%, 4.22% and 0.017% respectively. One can conclude, having these concentrations in mind, that SF₆ molecule can be found in nature mainly as ³²SF₆ and ³⁴SF₆. Sulfur hexafluoride has 15 vibrational degrees of freedom, or normal vibration modes. The most efficient absorption mode is ν₃ mode with characteristic frequency of 948cm⁻¹, or 10P (16) CO₂ laser line.

PHOTOACOUSTIC SPECTROSCOPY AND MULTIPHOTON ABSORPTION

During the past years many authors have advocated the photoacoustic technique (PA) as the simple, but powerful technique for IR linear and multiple photon (MPA) investigation [8-14]. Previously transmission spectroscopy (TRS) (a light attenuation technique) with a parallel or focused laser beam has been used [15,16], in spite of the limitations such as: difficulty to obtain long parallel laser beam of sufficient high intensity, difficulty to precisely determine the geometry and energy profile of a focused beam and necessity for very precise measurement of the excitation energy. On the other hand, the PA technique is simple, with high sensitivity and produces reproducible results under controlled experimental conditions. But it generally gives only relative measurements of MPA phenomena. Whenever the absolute values are needed, it is necessary to calibrate PA data with, e.g. a transmission technique (TRS), preferably within the same experiment and under the same conditions.

Recently, very detailed kinetic studies of infrared multiple photon absorption in SF₆ and SF₆-buffer gas (Ar in our case) mixtures, during a TEA CO₂ laser excitation have been published [33,34]. By using a time-resolved light attenuation technique, these authors have investigated the average number of photons absorbed per SF₆ molecule, the differential cross sections as function of time and fluence, as well as the vibrational, translational and rotational temperatures during the laser pulse.

The role of PA experiment here is to show that the SF₆ molecule is a really good absorber of IR radiation, which is very important for future global warming investigation. Working in nonlinear MPA regime is something that is not present, or present in a small number of cases, in our surroundings (atmosphere), but can easily show the physical characteristics concerning absorption and relaxation processes which can occur at the atmospheric pressure. However, it can be easily shown, that physical characteristics concerning absorption and relaxation processes which can occur on the atmospheric pressure, are much more obvious and thus easier to investigate on sub-atmospheric pressures. For a

comparison, the results for the same experimental conditions are taken from C₂H₄ + Ar measurements.

The sulfurhexafluoride (SF₆) molecule represents the most studied molecule from the point of view of multiple photon absorption (MPA) [9-14]. The effect of buffer-gas on MPA processes in SF₆ has also been extensively investigated [15-39]. The reason for this is that the SF₆ molecule is a suitable prototype molecule for such studies. So, its quantitative database has been established [9-14]. However, the interest in better understanding of the processes mentioned above is still present, for at least two reasons. First, investigation of this molecule enables one to understand important details of MPA processes themselves. Second, the relaxation processes caused by collisions with buffer-gas molecules and among absorbing polyatomic molecules (SF₆), especially in high excited vibrational states, are very important and should be investigated under controlled conditions [9-14].

At present, effects of collisions between a vibrationally excited molecule and particles of the buffer-gas in MPA processes are poorly understood. An increase in the absorption cross-section for infrared (IR) resonance radiation in the molecule (the effect of the enhanced absorption) with an increase in buffer-gas pressure has been observed in a few cases [16-39]. In some of these investigations, due to use of the high buffer-gas pressures and the high laser fluences, the authors have detected the average number of absorbed photons $\langle n \rangle$, which has exceeded drastically S-F bound energy, i.e. $\langle n \rangle$ was bigger than 33 [16,18,20,22].

It is common opinion that this increase in $\langle n \rangle$ is due to at least five important processes [13,16]. First, it is due to "rotational hole" filling effect that appears upon rotational relaxation, resulting in an increase of number of molecules that are excited effectively by the radiation. Second, it is due to the change of V-T relaxation processes. Third, it could be caused by a pressure broadening of rotational structures that would lead to an enhanced absorption of laser radiation within a greater range of frequencies. It is also caused by an inter-molecular and intra-molecular V-V transfer.

The main experimental parameter obtained and analyzed in this work is the total average number of absorbed photons $\langle n \rangle_{\text{total}}$ for SF₆ molecule surrounded with Ar as a buffer-gas species. Equation, used to calculate $\langle n \rangle_{\text{total}}$ values from the experimental PA parameters, valid for all types of gas mixtures, has a form [15-22]

$$\langle n \rangle_{\text{total}} = \frac{\Phi}{h\nu N l_m} \cdot \ln \left(1 - \frac{S(p, \gamma, T) P_a}{E_i} \right), \quad (1)$$

where $h\nu$ is laser photon energy, N is concentration of absorber in investigated gas mixture, l_m is length of photoacoustic microphone (detector) mounted inside the experimental cell, used to detect acoustic waves, E_i is incoming laser energy and $S(p, \gamma, T)$ is calibration sensitivity factor. $S(p, \gamma, T)$ is the function of gas sample pressure (p), characteristics of gas particles ($\gamma = c_p/c_v$) and temperature inside the experimental cell (T). This equation has two important characteristics that must be pointed out. First, as Eq.(1) is obtained from Lambert-Beer law, it shows that $\langle n \rangle_{\text{total}}$ corresponds to the average energy ($\langle E \rangle$) absorbed in the irradiated volume during the laser pulse ($\langle E \rangle = h\nu \langle n \rangle_{\text{total}}$). We must note that the value ($\langle E \rangle$) is not always equal to the average energy already stored in vibrational modes of absorbing molecules ($\langle E \rangle_v$), specially when working with long-tail pulses. Second, in the case of "top-hat" profile of the laser pulse, this equation gives the same value for $\langle n \rangle_{\text{total}}$ all over the irradiated volume, for constant pressure of investigated gas mixture during the laser pulse.

The base of the generalized coupled two-level (GCT) model is the coupled two-level absorber model described in details in Ref. [15,16]. This model contains the following features [15,16]. A finite bandwidth radiation field interacts with one of several rotational states of a molecule vibrational level, to promote transitions to an upper vibrational state. This interaction is considered in a rate equation approximation, resulting from direct spectral overlap of radiation field and the absorbing transition of the molecule. Other rotational states that are not coupled directly to the radiation field constitute a set of reservoir states that may be indirectly coupled to interacting rotational levels through collisions. Other vibrational levels that are coupled to the interacting states either by a collisional or collisionless inter-modal V-V' transfer process are also included in the reservoir states.

An approximate solution to differential equations, which describes the optical and collisional transitions among the four levels of the model (two absorber levels and two reservoir levels) is given [15,16] in the form

$$\frac{\langle n \rangle(\Phi)}{\langle f \rangle} = 1 - \exp\left(-\frac{\sigma_0 \Phi}{\langle f \rangle}\right), \quad (2)$$

which gives the ratio between the average number of absorbed photons per molecule $n(\Phi)$ and three variables: Φ (fluence), σ_0 (small-signal absorption cross section) and $\langle f \rangle$ (the effective fraction of the population for given vibrational transition which is coupled to the radiation field due to collisional relaxation process). In this equation, $n(\Phi)$ is not spatial average, but a local value that one can relate to the experimental values $\langle n \rangle_{\text{total}}$ through Eq.(1) in the case of "top-hat" spatial profile of used laser beam (our case). The approximate expression for $\langle f \rangle$ has a form [6]

$$\langle f \rangle = df_i \left\{ 1 - \exp\left[-\frac{f_r}{1-f_r} \cdot \frac{\tau_p}{\tau} \cdot \left(1 + \frac{f_i f_i}{\sigma_0 \Phi} \cdot \frac{\tau_p}{\tau}\right)\right]\right\} \cdot \left[1 - \exp\left(-\frac{\tau_p}{\tau}\right)\right] + df_r f_i \exp\left(-\frac{\tau_p}{\tau}\right), \quad (3)$$

where f_i is the fraction of molecules in the absorbing (usually ground) vibrational level ($f_i = 0.3$ for SF₆ at 300K), and f_r is the fraction of f_i molecules in the initial distribution that interacts directly with the radiation field. f_r can be obtained theoretically using simple relation $f_r = \Delta_L F(\nu)$, where Δ_L is laser line width and $F(\nu)$ is absorption distribution function for given absorbing molecule and defined experimental conditions [15,16]. The quantity d is defined as

$$d = \frac{\beta}{1+\beta}, \quad (4)$$

where β is the ratio of degeneracy of the upper and lower vibrational levels, τ_p is laser pulse duration and τ is equilibration time of the absorber level and reservoir level, usually taken as rotational relaxation time in previous investigation [15,18,20].

This model is valid in three limiting cases: 1) weak coupling (collisionless), when $(\tau_p / \tau) < 1$; 2) strong coupling (collisional) when $(\tau_p / \tau) > 1$ and low flux $((\sigma_0 \Phi \tau) / (f_i f_i \tau_p) < 1)$; 3) strong coupling (collisional) when $(\tau_p / \tau) > 1$ and high flux $((\sigma_0 \Phi \tau) / (f_i f_i \tau_p) > 1)$. But, this model, because of such normalization procedure, is not valid in the case of infrared multiphoton absorption (IRMPA processes) when $\Phi > \Phi_s$, where Φ_s is a IRMPA starting fluence. Then two-level approximation brakes down. Problem lays in the fact that Eq.(2)

predicts that $n(\Phi)$ approaches a constant value at high fluence. Experimental results show that $n(\Phi)$ continues to increase in large polyatomic molecules. Knowing these problems, generalization of coupled two-level model was done [15,16]. Briefly, if one assumed that the dynamic of the molecule-radiation field is, in first approximation, controlled by the lower vibrational level of the absorbing transition, then generalized Eq.(2) can be written in normalized functional form, taking the limit $\beta \rightarrow \infty$, as [15,16]

$$\frac{n(\Phi)}{\langle f \rangle} = G \left(\frac{\sigma_0 \Phi}{\langle f \rangle} \right), \quad (5)$$

which is valid for $((\sigma_0 \Phi) / \langle f \rangle) > 1$, and approaches two-level result in Eq.(2) for $((\sigma_0 \Phi) / \langle f \rangle) < 1$. Experiments show that, in case of SF₆, $G((\sigma_0 \Phi) / \langle f \rangle) \rightarrow ((\sigma_0 \Phi) / \langle f \rangle)^{2/3}$ in high-fluence regime, e.g. when $((\sigma_0 \Phi) / \langle f \rangle) > 1$. Knowing that, for the collisional and high-fluence regime, Eq.(3) can be written in the form [15,16]

$$f = f_i \cdot \left[1 - \exp \left(\frac{-f_r}{1-f_r} \cdot \frac{\tau_p}{\tau} \right) \right], \quad (6)$$

while Eq.(5), in our case, is

$$\langle n \rangle_{\text{total}} (p_{\text{buff.}}, \Phi) = \langle f \rangle^{1/3} (\sigma_0 \Phi)^{2/3} = \left\{ f_i \left[1 - \exp \left(\frac{-f_r}{1-f_r} \cdot \frac{\tau_p}{\tau} \right) \right] \right\}^{1/3} \cdot (\sigma_0 \Phi)^{2/3}, \quad (7)$$

where, concerning our experimental conditions e.g. "top-hat" profile and quality of our laser beam, $n(\Phi)$ in Eq.(5) is equal to $\langle n \rangle_{\text{total}}$ in Eq.(1). The equation (7) is the main equation obtained with GCT model to be utilized in our investigation.

Let us analyze the IRMPA processes during the laser pulse in collisionless and collisional regime. Generally speaking, if there is no collision between absorbing molecules (or absorbing molecules and buffer-gas particles) only the laser fluence Φ is responsible for the excitation level of the absorbing molecule, and one can write that $\langle n \rangle_{\text{total}} = \langle n \rangle_{\Phi}$. But collisions play very important role in IRMPA processes. They can repopulate preferentially pumped ro-vibrational states and broaden the absorption lines of the absorbing molecule (mainly through rotational relaxation) and also deactivate excited molecules (mainly through V-T relaxation), allowing them to absorb more photons during the laser pulse. Knowing that, it is possible to write simple expression for $\langle n \rangle_{\text{total}}$ in the form

$$\langle n \rangle_{\text{total}} = \langle n \rangle_{\Phi} + \langle n \rangle_{\text{coll.}}, \quad (8)$$

or

$$\langle n \rangle_{\text{total}} = \langle n \rangle_{\Phi} + \langle n \rangle_{\text{rot.}} + \langle n \rangle_{\text{V-T}} + \langle n \rangle_{\text{V-V}}, \quad (9.a)$$

assuming that $\langle n \rangle_{\text{coll.}} = \langle n \rangle_{\text{rot.}} + \langle n \rangle_{\text{V-T}} + \langle n \rangle_{\text{V-V}}$. $\langle n \rangle_{\text{rot.}}$, $\langle n \rangle_{\text{V-T}}$ and $\langle n \rangle_{\text{V-V}}$ represent partial values of $\langle n \rangle_{\text{coll.}}$. Originating from collisionally induced rotational relaxation (R, R-T), vibrational to translational (V-T) and intermolecular vibrational to vibrational (V-V) relaxation of absorbing molecules (SF₆) respectively, during the laser pulse. When we talk about rotational relaxation we assume, so called, positive relaxation in the manner of its influence on photon absorption. Such process, keeping the absorbed photons inside the ro-vibrational modes of molecule, is rotation-to-rotation (R-R) relaxation. Also, rotational

to translational (R-T) process is present too, but, according to our experimental conditions, its influence on multiphoton absorption is much lower, in comparison with R-R processes. Possible intermolecular V-V relaxation process occurs only in the case of molecular buffer-gas, and its existence strongly depends on experimental conditions. In the case of atomic and most of molecular buffers, this process can be neglected, and Eq.(9.a) can be written in the form

$$\langle n \rangle_{\text{total}} = \langle n \rangle_{\Phi} + \langle n \rangle_{\text{rot.}} + \langle n \rangle_{\text{v-T}}, \quad (9.b)$$

or, knowing that $\langle E \rangle = h\nu \langle n \rangle$,

$$\langle E \rangle = \langle E \rangle_{\text{total}} = \langle E \rangle_{\Phi} + \langle E \rangle_{\text{rot.-rel.}} + \langle E \rangle_{\text{v-T}} = \langle E \rangle_{\text{v}} + \langle E \rangle_{\text{t}}, \quad (9.c)$$

where $\langle E \rangle_{\text{v}} = \langle E \rangle_{\Phi} + \langle E \rangle_{\text{rot.}}$ represents the average energy stored in the irradiated ensemble of absorbing molecules, and $\langle E \rangle_{\text{t}} = \langle E \rangle_{\text{v-T}}$ represents the average energy released from the absorber ensemble, stored in the translational modes of gas mixture colliding partners (mostly buffer-gas species).

In this work we will show that, using GCT model (Eq.(7)), it is possible to obtain all physical quantities appearing in Eqs.(8) and (9.a,b,c) directly, or using some of PAS results obtained by TROA, TRA and SA methods [20, 22]), as the functions of laser fluence, buffer-gas pressure and small-signal absorption cross section σ_0 . This will give us a clear view of what are the mechanisms of the laser field energy entering into the irradiated system, and what are the most important collisional processes which contribute to absorption the most.

Basic idea consists of following [22]. Using pulsed PAS technique it is possible to obtain, experimentally, $\langle n \rangle_{\text{total}}$ values using Eq.(1), as a function of the buffer-gas pressure at constant laser fluence Φ . Now these results can be fitted using the final result of GCT model, with functional form based on Eq.(7), given as

$$\langle n \rangle_{\text{total}}(p_{\text{buff.}}, \Phi) = \{[1 - \exp(-a \cdot p_{\text{buff.}})]b\}^{1/3} \cdot (\sigma_0 \Phi)^{2/3}, \quad (10)$$

assuming that f_i , σ_0 and Φ are already known. However, a and b are fitting parameters. Analyzing this equation it is obvious that it consists of two parts which represent different influences on the multiphoton absorption process: first part $\{[1 - \exp(-ap_{\text{buff.}})]b\}$ f_i presents the pressure influence of investigated gas mixture (in most cases pressure of the buffer gas, because this pressure is much larger than the pressure of absorbing molecules), and second part presents the influence of laser fluence ($\sigma_0 \Phi$). Comparing Eq.(6) and Eq.(10) it is obvious that

$$ap_{\text{buff.}} = \frac{f_i}{1-f_i} \cdot \frac{\tau_p}{\tau}. \quad (11)$$

Because not only R-R and R-T but also V-T relaxation is responsible for finally obtained value of $\langle n \rangle_{\text{total}}$, we must take that $\tau = \tau_{\text{coll}}$, where τ_{coll} . ($\tau_{\text{coll}}^{-1} = Z$ - total number of collisions per second) includes all average lifetimes of all possible collisional processes between molecular absorber and buffer-gas species. Then all types of collisions have the influence on $\langle n \rangle_{\text{total}}$ value.

On the other hand, if one wants to obtain partial values of $\langle n \rangle_{\text{total}}$ depending only on buffer-gas pressure, GCT model can be used substituting τ with one of relaxation times corresponding to dominant collisional process for given experimental conditions. These relaxation times must be obtained with some other spectroscopic technique. In our case we have obtained, independently, relaxation times τ for all of possible collisional processes, such as: rotational to rotational (τ_{rot}), vibrational to vibrational ($\tau_{\text{V-V}}$) and vibrational to translational ($\tau_{\text{V-T}}$) relaxation, dependent on the type of buffer-gas species and pressure of absorbing molecules. In the case of low molecular absorber partial pressure and atomic types of buffer-gas species, it is sufficient to know only τ_{rot} and $\tau_{\text{V-T}}$, since only these processes are present. In such case we adopt some of PAS methods, using the obtained PAS experimental results. These methods are TROA and TRA for V-T relaxation time determination ($\tau_{\text{V-T}}$), and SA method for rotational to rotational relaxation time determination (τ_{rot}). They give the necessary relaxation times directly. Knowing these parameters ($\tau_{\text{V-T}}$ and τ_{rot}), Eq.(10) can be written in the general form suitable for $\langle n \rangle_{\text{rot}}$ or for $\langle n \rangle_{\text{V-T}}$

$$\langle n \rangle_k(p_{\text{buff}}, \Phi) = \left\{ \left[1 - \exp\left(-a \cdot \frac{\tau_{\text{coll}}}{\tau_k} \cdot p_{\text{buff}}\right) \right] \cdot b \right\}^{1/3} \cdot f_i^{1/3} \cdot (\sigma_0 \Phi)^{2/3}, \quad (12)$$

where k subscript corresponds to rot. or V-T, indicating which process one would like to analyze.

Concerning the fitting parameter b , it is connected with the maximal fraction of absorbing molecules (SF₆ in our case) which are directly coupled with laser radiation field inside the irradiated volume, due to collisions between absorbing and non-absorbing gas-mixture species. We will denote this parameter as $f_{\text{coll.max}}$. Then we can write that the fraction of the molecules, inside the laser beam volume directly coupled to the radiation field due to collisions, is $\{[1 - \exp(-ap_{\text{buff}})]b\}f_i = f_{\text{coll}}$. and, concerning Eq.(6), $f_{\text{coll}} \equiv \langle f \rangle$ [22]. On the other hand, value $1 - f_{\text{coll.max}}$ is equal to f_{Φ} representing the fraction of absorbing molecules which are coupled with radiation field due to the influence of laser fluence. Using now Eqs.(12) and (8) it is possible to calculate all partial values of $\langle n \rangle_{\text{total}}$, which allows one to understand the details and dynamics of IRMPA processes inside the irradiated volume during the laser pulse.

RESULTS AND DISCUSSION

Let us compare the results for total average number of absorbed photons $\langle n \rangle_{\text{total}}$ for SF₆ molecule (Figure 1) and C₂H₄ molecule (Figure 2) as a function of buffer-gas Ar pressure p_{Ar} , for the same laser fluence and spatial and temporal laser beam characteristics.

It is obvious from both figures that $\langle n \rangle_{\text{total}}$ values (analyzed with GCT model, full line, Figure 1) for SF₆ molecule are much higher than in the case of C₂H₄. It means that SF₆ absorption capabilities are much larger, giving it an opportunity to absorb radiation field photons on higher pressures with the same efficiency (constant value of $\langle n \rangle_{\text{total}} = f(p_{\text{Ar}})$ for $p_{\text{Ar}} > 50$ mbar). Extrapolation of these results leads us to the conclusion that similar SF₆ behavior can be expected on the atmospheric, too. This is the reason why sulfur hexafluoride is one of the potentially most dangerous greenhouse gases, found to

be indirectly responsible for many physical and chemical reactions and having a great influence on global warming.

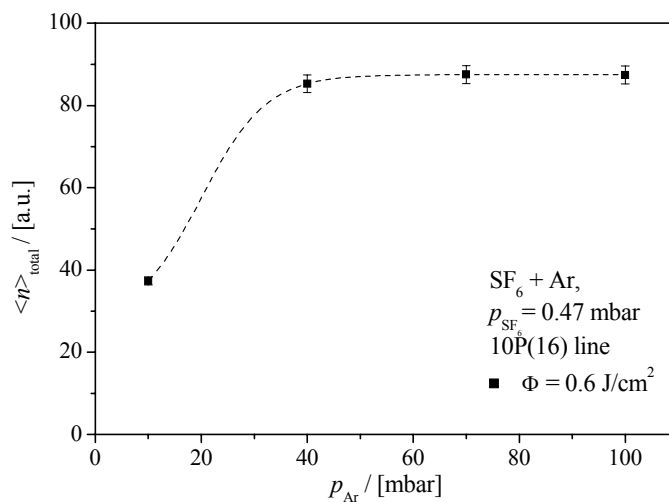


Fig. 1. Total average number of absorbed photons $\langle n \rangle_{\text{total}}$ for SF₆ molecule as a function of Ar buffer-gas pressure p_{Ar} for SF₆+Ar mixture, under constant laser fluence $\Phi = 0.6 \text{ J/cm}^2$, at 10P(16) line.

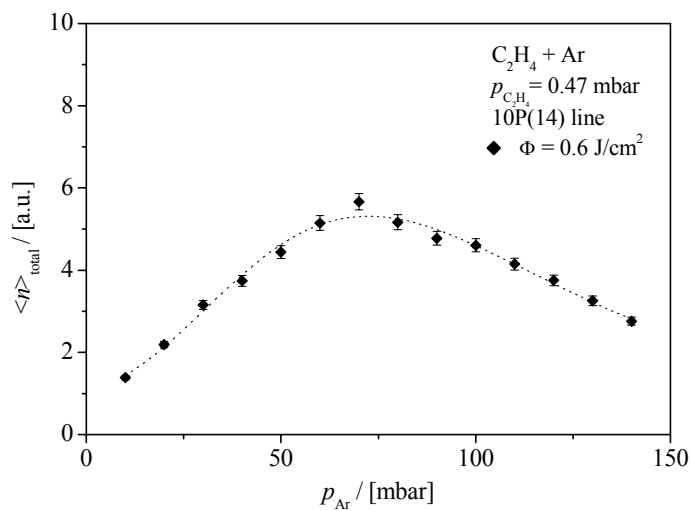


Fig. 2. Total average number of absorbed photons $\langle n \rangle_{\text{total}}$ for C₂H₄ molecule as a function of Ar buffer-gas pressure p_{Ar} for C₂H₄+Ar mixture, under constant laser fluence $\Phi = 0.6 \text{ J/cm}^2$, at 10P(14) line.

Analyzing ethylene (C₂H₄) in Figure 2, one can see that its $\langle n \rangle_{\text{total}}$ value reaches maximum at $p_{\text{Ar}} \sim 70$ mbar. After that $\langle n \rangle_{\text{total}}$ decreases, and function $\langle n \rangle_{\text{total}} = f(p_{\text{Ar}})$ tends to reach linear absorption regime ($\langle n \rangle_{\text{total}} \sim 1$) for $p_{\text{Ar}} > 140$ mbar.

In Figure 3, both $\langle n \rangle_{\text{total}} = f(p_{\text{Ar}})$ for SF₆ and C₂H₄ graphs are given together (from Figures 1 and 2) providing a clear view on molecules' behavior in gases and in the presence of strong radiation field. It is very important also to see, collisional influence on both molecules (Ar pressures lower than 50 mbar) where we have positive influence of collisions on molecules absorption characteristics (enhanced absorption) due to rotational relaxation processes. On higher argon pressures (> 60 mbar) vibrational to relaxational (V-T) process starts to dominate. In the case of SF₆ molecule, the balance starts to occur between excitation and V-T relaxation processes, producing constant $\langle n \rangle_{\text{total}}$ values. From this behavior one can also conclude that SF₆ molecule is a very good energy transfer partner, allowing very fast and efficient energy transfer from its vibrational modes to translational modes of its collisional partners. In the case of ethylene, that relaxation and energy transfer capabilities are not at such high level as they are in the case of SF₆. Those physical characteristics of absorbing molecules are very important to know and analyze, especially in the case of climate modeling and understanding of global warming and greenhouse effect.

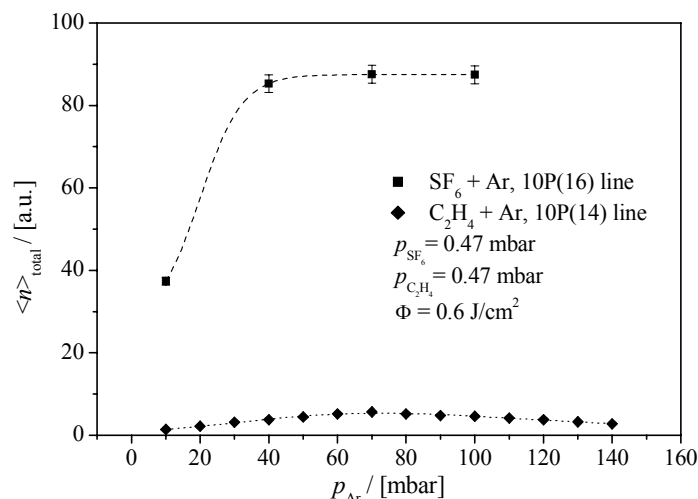


Fig. 3. Comparison of total average number of absorbed photons $\langle n \rangle_{\text{total}}$ for SF₆ and C₂H₄ molecule as a function of Ar buffer-gas pressure p_{Ar} , for SF₆+Ar and C₂H₄+Ar mixtures, under constant laser fluence $\Phi = 0.6 \text{ J/cm}^2$, at 10P(16) and 10P(14) line respectively.

Acknowledgements. *This work was done as a part of the activities within the frame of 141015 Project of the Ministry of Science and Environmental Protection of the Republic of Serbia and World Year of Physics 2005 activities supported by Serbian and European Physical Society. Also, the realization of this experiment was part of the Memorandum of Understanding between Physics Professors Association from Mathematical high school in Beograd and Laboratory for Atomic, Molecular and Laser Spectroscopy from the Institute of Physics in Beograd-Zemun, based on the Ministry of Education and Sport of the Republic of Serbia young talents search and support activities.*

REFERENCES

1. FCCC (1996) Framework Convention on Climate Change; FCCC/CP/1996/15/Add.1; 29 October 1996; Report of the Conference of the Parties at its second session. Revised Guidelines for the Preparation of National Communications by Parties Included in Annex 1 to the Convention, p18. Geneva 1996.
2. IPCC (2001) *Climate Change 2001: A Scientific Basis*, Intergovernmental Panel on Climate Change; J.T. Houghton, Y. Ding, D.J. Griggs, M. Noguer, P.J. van der Linden, X. Dai, C.A. Johnson, and K. Maskell, eds.; Cambridge University Press. Cambridge, U.K.
3. IPCC (2000) Good Practice Guidance and Uncertainty Management in National *Greenhouse Gas Inventories*. IPCC National Greenhouse Gas Inventories Programme Technical Support Unit, Kanagawa, Japan. Available online at <<http://www.ipcc-ggip.iges.or.jp/gp/report.htm>>.
4. IPCC (1999) *Aviation and the Global Atmosphere*. Intergovernmental Panel on Climate Change; Penner, J.E., et al., eds.; Cambridge University Press. Cambridge, U.K.
5. IPCC (1996) *Climate Change 1995: The Science of Climate Change*. Intergovernmental Panel on Climate Change; J.T. Houghton, L.G. Meira Filho, B.A. Callander, N. Harris, A. Kattenberg, and K. Maskell, eds.; Cambridge University Press. Cambridge, U.K.
6. IPCC/UNEP/OECD/IEA (1997) Revised 1996 IPCC Guidelines for National *Greenhouse Gas Inventories*. Paris: Intergovernmental Panel on Climate Change, United Nations Environment Programme, Organization for Economic Co-Operation and Development, International Energy Agency.
7. UNEP/WMO (2000) *Information Unit on Climate Change*. Framework Convention on Climate Change (Available on the internet at <<http://www.unfccc.de>>.)
8. WMO (1999) Scientific Assessment of Ozone Depletion, Global Ozone Research and *Monitoring Project-Report No. 44*, World Meteorological Organization, Geneva, Switzerland.
9. Амбарцумян Р. В., Макаров Е. А., Пурецкий А. А., *Письма в ЖЭТФ*, **28**, (1978) 246
10. Баграташвили Р. Н., Должиков В. С., Летохов В. С., *ЖЭТФ*, **76**, (1979) 18
11. Ambartzumian R. V., Chekalin N. V., Gorokhov Yu. A., Letokhov V. S., Makarov G. N., Ryabov E. A., in *Lasers Spectroscopy II*, Eds. Garoche S. et al., Lecture Notes in Physics, Berlin-Heidelberg-New York; Springer-Verlag, **43**, (1975) 121
12. Bagratashvili V. N., Vainer Y. G., Doljnikov V. D., Letokhov V. S., Makarov A. A., Maliavkin L. P., Ryabov E.A., Sil'kis A. C., *Optics Lett.*, **6**, (1981) 148
13. В.С. Летохов, в *Нелинейные селективные фотопроецессы в атомах и молекулах*, Наука, Москва (1983)
14. Y.R. Shen, in *The Principles of Nonlinear Optics*, John Wiley & Sons, Inc., (1984)
15. J.L. Lyman, G.P. Quigley and O.P. Judd, in *Multiple-Photon Excitation and Dissociation of Polyatomic Molecules*, Ed. C.D. Cantrell, Springer-Verlag, Berlin, (1986), 9
16. O.P. Judd, *Chem. Phys.*, **71**, (1979), 4515
17. J. Jovanović-Kurepa, M. Terzić, D. D. Markušev and P. Vujković Cvijin, *Meas. Sci. Technol.*, **5**, (1994) 847
18. J. Jovanović-Kurepa, D.D. Markušev, M. Terzić and P. Vujković Cvijin, *Chem. Phys.*, **211**, (1996) 347
19. K.M. Beck, A. Ringwelski and R.J. Gordon, *Chem Phys. Lett.*, **89**, (1985) 529
20. D.D. Markušev, J. Jovanović-Kurepa, J. Slivka, M. Terzić, *J.Q.S.R.T.*, **61**, (6) (1999) 825
21. R.J. Gordon and K.M. Beck, *J. Chem Phys.*, **89**, (1988) 5560
22. D.D. Markušev, J. Jovanović-Kurepa, M. Terzić, *J.Q.S.R.T.*, **76**, (1) (2003) 85
23. F.M. Lussier, J.I. Steinfeld, T.F. Deutsch, *Chem. Phys. Lett.*, **58**, (1978) 277
24. D.G. Sutton, T. Burak, J.I. Steinfeld, *IEEE J. of Quantum Electron.*, **QE-7** (1971) 82
25. M. Terzić, D.D. Markušev, J. Jovanović-Kurepa, *J. Phys. B: At. Mol. Opt. Phys.*, **32** (1999) 1193
26. M. Terzić, D.D. Markušev, J. Jovanović-Kurepa, *Chem. Phys.*, **270** (2) (2001) 383
27. D.D. Markušev, J. Jovanović-Kurepa, M. Terzić, *Rev. Sci. Instrum.*, **74**, Issue 1, (2003), 303
28. M. Terzić, D.D. Markušev, J. Jovanović-Kurepa, *Rev. Sci. Instrum.*, **74**, Issue 1, (2003), 322
29. M. Lenzi, E. Molinari, G. Piciacia, V. Sessa and M.L. Terranova, *Chem. Phys.*, **108**, (1986) 167
30. M. Lenzi, E. Molinari, G. Piciacia, V. Sessa and M.L. Terranova, *Chem. Phys.*, **142**, (1990) 473
31. C. Angelie, P. Millie, *Chem. Phys.*, **82**, (1983) 171
32. C. Angelie, R. Capitini and P. Girard, in *Multiphoton Processes*, Ed. S.J. Smith and P.L. Knight, Cambridge University Press, (1988) 226
33. D.D. Markušev, M. Rabasović, M. Terzić and J. Jovanović-Kurepa, *J. de Phys. IV*, **125**, (2005), 23
34. Mira Terzić, Dragan D. Markušev and Mihajlo Rabasović, *J. de Phys. IV*, **125**, (2005), 55
35. M. W. Sigrist, in *Air Monitoring by Spectroscopy Techniques*, *Chem. Anal.* **127**, edited by M. W. Sigrist, John Wiley & Sons, Inc., New York, (1994); Chapter 4.
36. M. W. Sigrist, *J. Appl. Phys.*, **60**, (1986), 83.
37. M.W. Sigrist and C. Fischer, *J. de Phys. IV*, **125**, (2005), 619
38. S.S. Mitra and S.S. Bhattacharyya, *J. Phys. B: At. Mol. Opt. Phys.*, **25**, (1992), 2535
39. S.S. Mitra and S.S. Bhattacharyya, *J. Phys. B: At. Mol. Opt. Phys.*, **27**, (1994), 1773

GLOBALNO ZAGREVANJE I MOLEKUL SF₆**Jelena Gajević, Marija Stević, Jelena Nikolić,
Mihailo Rabasović, Dragan Markušev**

U ovom radu je dat kratak prikaz osnovnih fizičkih karakteristika molekula SF₆ i njegov potencijalni uticaj na globalno zagrevanje i efekat staklene bašte. Ispitivane su njegove apsorpcione i relaksacione osobine u okviru nelinearnih interakcija molekula apsorbera sa jakim laserskim poljem u različitim gasnim smešama. Svi eksperimenti rađeni su na različitim pritiscima smeše da bi se dobili odgovarajući rezultati koji karakterišu i relaksacione osobine apsorbera, i njegove mogućnosti prenosa energije na ostale gasne partnere. Da bi se na konkretnom primeru pokazale osobine dobrog apsorbera infracrvenog zračenja na različitim pritiscima, izvršena su poređenja rezultata dobijenih multifotonskom apsorpcijom molekula SF₆ i molekula C₂H₄ u smeši sa argonom pod istim eksperimentalnim uslovima. Sva merenja prikazana u ovom radu dobijena su korišćenjem impulsne fotoakustičke spektroskopije prilagođene za merenja u gasnim smešama na podatmosferskim i atmosferskom pritisku.